eLIFE elifesciences.org

RESEARCH ARTICLE

Figures and figure supplements

Lmx1b is required at multiple stages to build expansive serotonergic axon architectures

Lauren J Donovan *et al*

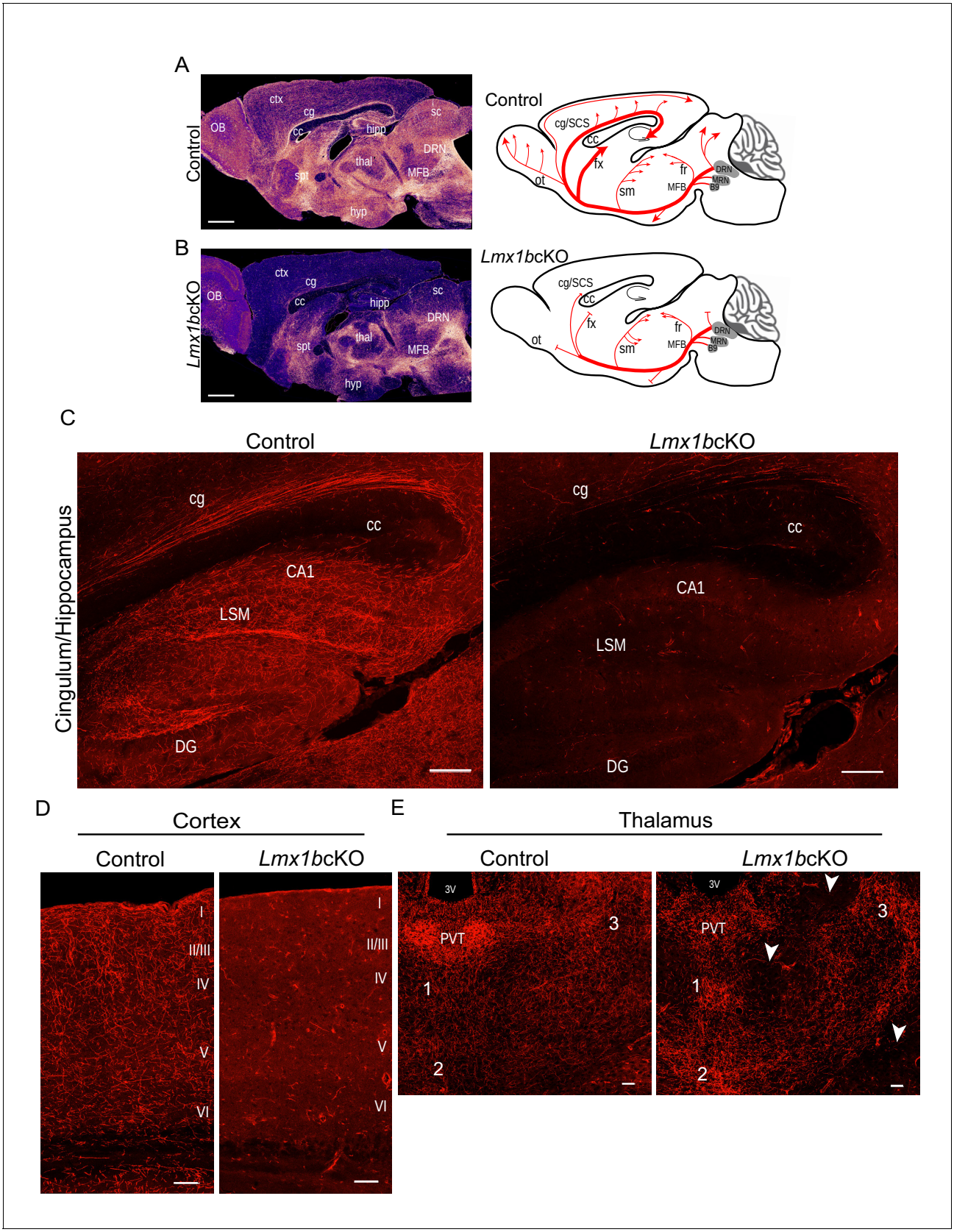

Figure 1. Lmx1b is required for the formation of ascending 5-HT axon projection pathways. (**A, B**) Ascending 5-HT axonal projection system immunolabeled using an anti-RFP antibody to TdTomato in whole sagittal forebrain sections of 3 month old mice displayed by heatmap. *Lmx1b*cKO

Figure 1 continued on next page

Figure 1 continued

TdTomato$^+$ axons were nearly absent in numerous brain regions (**B**) compared to controls (**A**) (n = 6, controls; n = 7, *Lmx1b*cKO adult mice). *Right*, schematics depicting 5-HT axon trajectories in *Lmx1b*cKO vs. control brains. Scale bars, 1000 μm. OB, olfactory bulb; ctx, *cortex*; cg, *cingulum*; cc, *corpus callosum*; hipp, *hippocampus*; spt, *septum*; hyp, *hypothalamus*; thal, *thalamus*; sc, *superior colliculus*; MFB, *medial forebrain bundle*; DRN, *dorsal raphe nucleus*. Schematic (*right*): ot, *olfactory tract*; cg/SCS, *cingulum/supracallosal stria*; fx, *fornix*; sm, *stria medularis*; fr, *fasciculus retroflexus*. (**C**) Confocal images of TdTomato$^+$ axons in sagittal sections. *Lmx1b*cKO axons failed to fill cingulum bundles or innervate the hippocampus. Scale bars, 200 μm. cg, *cingulum*; cc, corpus callosum; LSM, *lacunosum moleculare*; DG, *dentate gyrus*; CA1 of hippocampus. (**D**) Coronal sections of cortex show near complete lack of *Lmx1b*cKO TdTomato$^+$ axons Scale bars, 50 μm. (**E**) Coronal view of altered patterns of TdTomato$^+$ axons in *Lmx1b*cKO thalamus. Arrowheads indicate areas devoid of axons in *Lmx1b*cKO thalamus. Numbers correspond to areas of axon clumping in *Lmx1b*cKO thalamus. See ***Figure 1—figure supplement 2*** for high magnification images. Scale bars, 100 μm. PVT, *paraventricular nucleus of the thalamus*; 3V, *third ventricle*.

DOI: https://doi.org/10.7554/eLife.48788.002

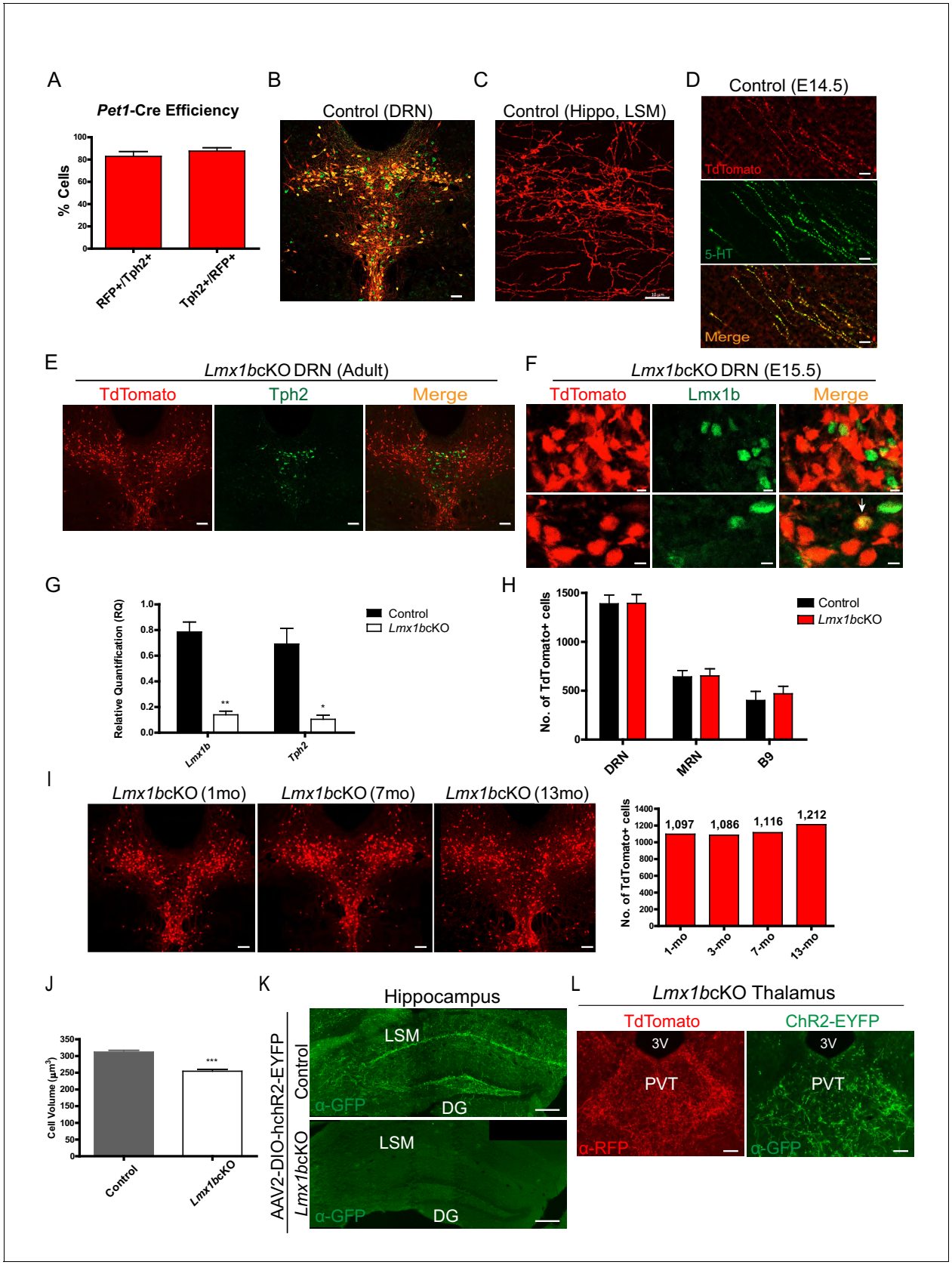

Figure 1—figure supplement 1. Surrogate marking of 5-HT cell bodies and axons and Lmx1b conditional targeting. (**A**) *Pet1-Cre* efficiency: 82% Tph2 + cells expressed TdTomato+ (RFP+/Tph2+) and 88% of TdTomato+ cells expressed Tph2 (Tph2+/RFP+) (n = 2 control mice). Data are represented as

Figure 1—figure supplement 1 continued on next page

Figure 1—figure supplement 1 continued

mean ± SEM. (**B**) TdTomato+ cells co-labeled with serotonergic marker Tph2 in the DRN. Immunofluorescence of Tph2 (green) and TdTomato (red). Scale bars, 100 μm. (**C**) TdTomato+ axons were found throughout the adult brain. Lacunosum moleculare layer (LSM) of hippocampus shown here. Scale bars, 10 μm. (**D**) Co-immunolabeled axons at embryonic day (**E**) 14 with anti-5-HT and anti-RFP antibodies. Scale bars, 20 μm. (E) A majority of TdTomato+ *Lmx1b*cKO mutant cells did not co-localize with Tph2 (n = 6, control; n = 7, *Lmx1b*cKO; 2.5–3.5 month old mice). Scale bars, 100 μm. (**F**) A majority of TdTomato+ *Lmx1b*cKO mutant cells did not co-localize with Lmx1b protein (E15.5 shown). A small number of cells were TdTomato^{+} and Lmx1b^{+} (bottom row, arrow). Scale bars, 5 μm. (**G**) RT-qPCR of *Lmx1b* and *Tph2* in flow sorted YFP+ cells from control and *Lmx1b*cKO E17.5 embryos (n = 4, control; n = 4, *Lmx1b*cKO embryos). Unpaired t-test with Welch's correction, *p<0.05, **p<0.001, and ***p<0.0001. Data are represented as mean ± SEM. (**H**) Counts of TdTomato+ cells in *Lmx1b*cKO mice did not differ from controls. Every 4th section counted throughout DRN/MRN/B9 raphe nuclei (n = 3 mice/genotype). Data are represented as mean ± SEM. (**I**) *Lmx1b*cKO cell bodies survive at least up to 13 months. Counts of TdTomato+ neurons in 6 matched sections for each animal (*right*) (n=1 animal per time point; 1mo, 3mo, 7mo, 13mo). Scale bars, 100μm. (I) *Lmx1b*cKO cell bodies survive at least up to 13 months. Counts of TdTomato+ neurons in 6 matched sections for each animal (*right*) (n=1 animal per time point; 1mo, 3mo, 7mo, 13mo). Scale bars, 100μm. (**J**) Volume of *Lmx1b*cKO cell bodies were significantly smaller than controls (n = 587 control cells; n = 442 *Lmx1b*cKO cells). Unpaired t-test with Welch's correction, *p<0.05, **p<0.001, and ***p<0.0001. Data are represented as mean ± SEM. (**K, L**) Expression of a YFP tagged channel rhodopsin by AAV2 viral injection to DRN/MRN of *Lmx1b*cKO and control mice. No YFP expression was found in *Lmx1b*cKO hippocampus (**K**) while YFP-labeled axons co-localized with TdTomato in the *Lmx1b*cKO thalamus (**L**). Scale bars, 200 μm (K), 50 μm (L).

DOI: https://doi.org/10.7554/eLife.48788.003

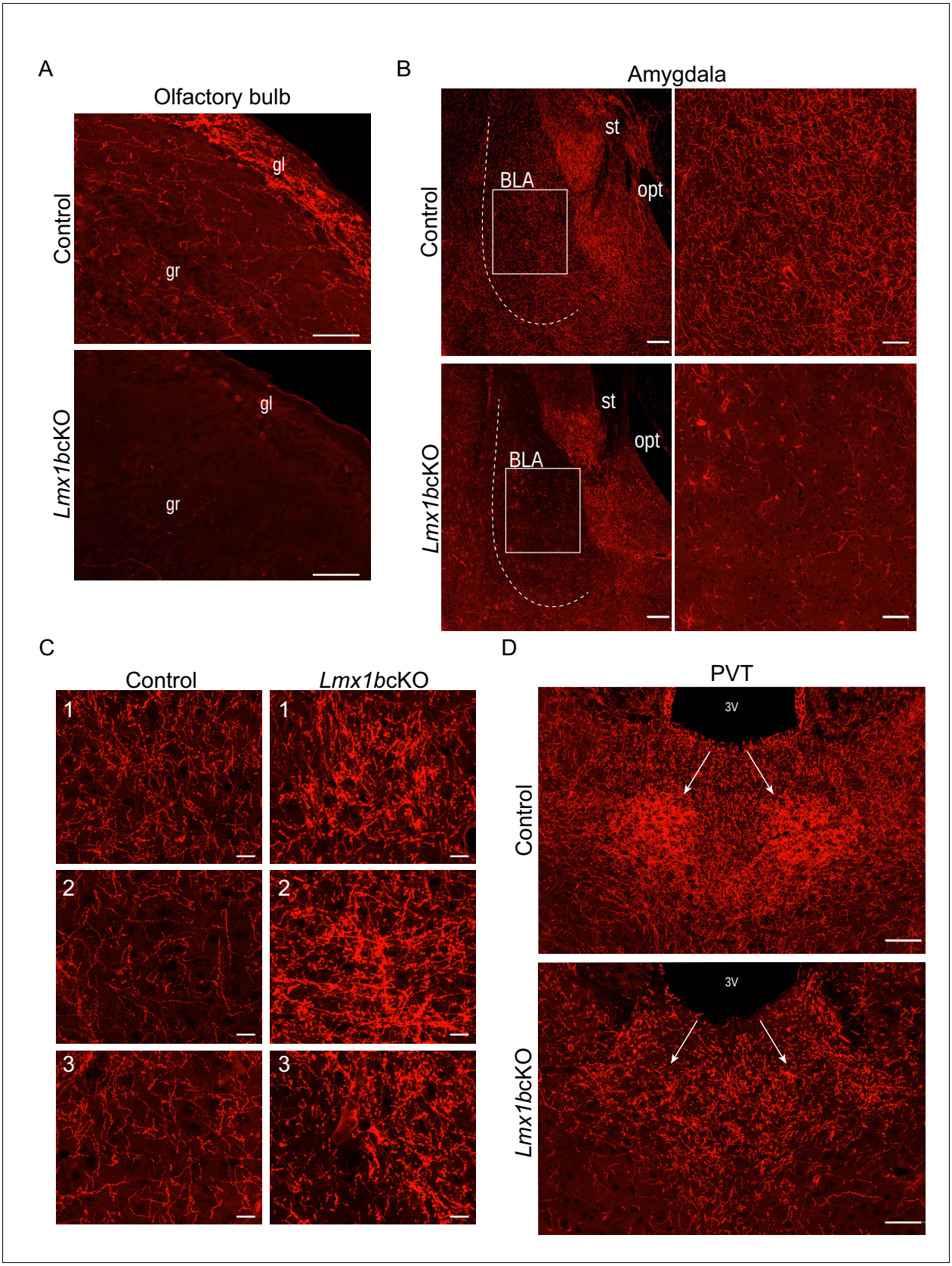

Figure 1—figure supplement 2. Lmx1b deficiency disrupts 5-HT axon patterns in the forebrain. (**A**) Sagittal sections of olfactory bulb show near complete lack of *Lmx1b*cKO TdTomato+ axons. Scale bars, 50 μm. gl, *glomerular layer*; gr, *granule layer*. (**B**) TdTomato+ axons severely reduced

Figure 1—figure supplement 2 continued on next page

Figure 1—figure supplement 2 continued

throughout *Lmx1b*cKO amygdala compared to controls (BLA, *shown right*). Scale bars, 100 μm. BLA, *basolateral amygdala*; st, *stria terminalis*; opt, *optic tract*. (**C**) High magnification showing areas of clumping (correlate to numbers in ***Figure 1E***) found in *Lmx1b*cKO thalamus compared to controls. Scale bars, 20 μm. (**D**) Lack of TdTomato+ axons in the PVT of *Lmx1b*cKO mice. Scale bars, 50 μm. 3V, *third ventricle*; PVT, *paraventricular nucleus of the thalamus*.

DOI: https://doi.org/10.7554/eLife.48788.004

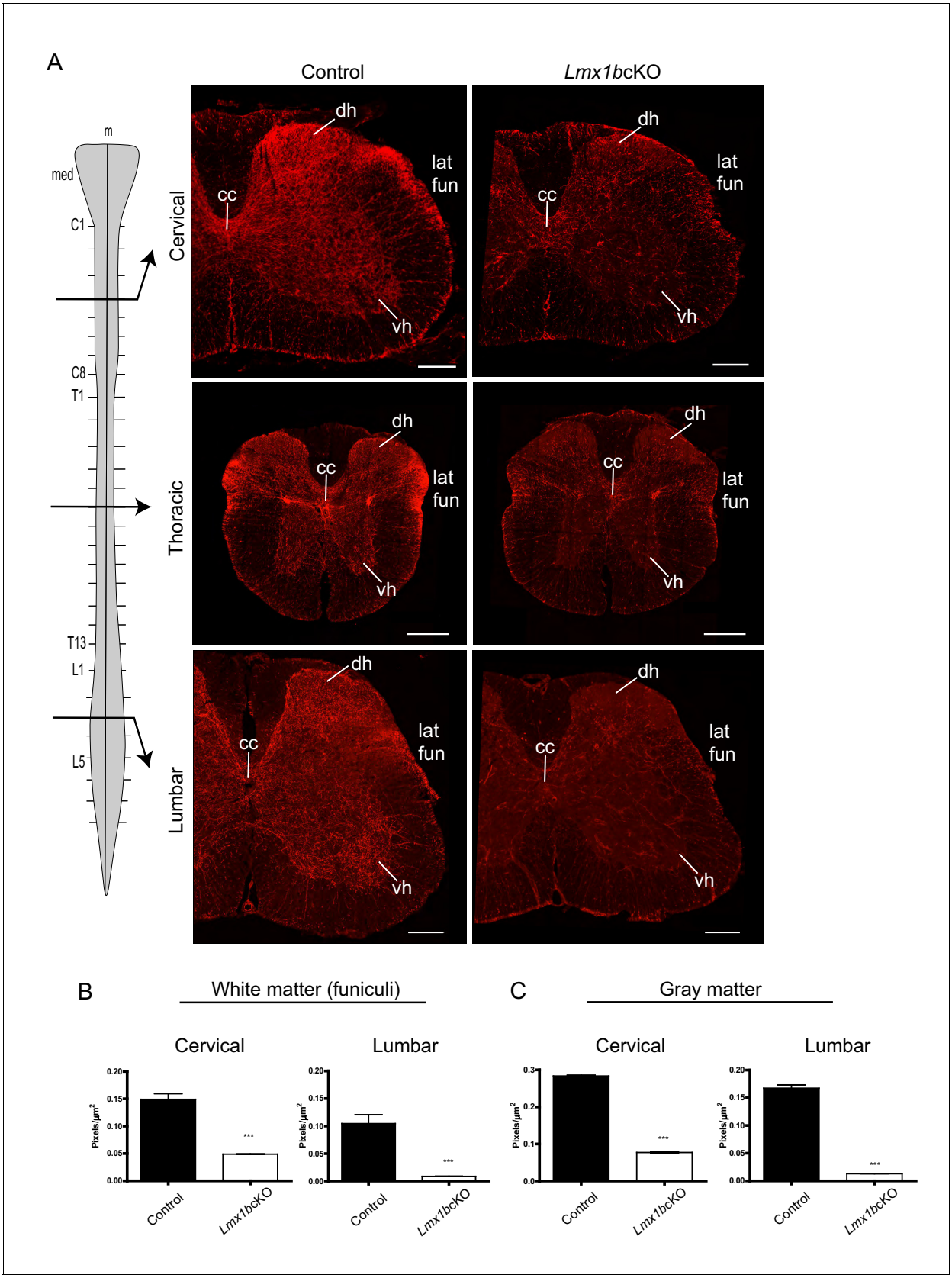

Figure 2. Lmx1b is required for the formation of descending 5-HT axon projection pathways. (**A**) Coronal sections taken at cervical (C4), thoracic (T6), and lumbar (L3) levels of the spinal cord (diagram, *left*). Immunolabeling for TdTomato shows *Lmx1b*cKO axons were severely reduced at every level of

Figure 2 continued on next page

Figure 2 continued

the cord in both gray and white matter compared to controls. Scale bars, 200 μm. m, *midline*; med, *medulla*; cc, *central canal*; dh, *dorsal horn*; vh, *ventral horn*; lat fun, *lateral funiculi*. (**B, C**) Quantification of total TdTomato^{+} axons (pixels/μm^{2}) in white (**B**) and gray (**C**) matter at cervical and lumbar levels (n = 3, control; n = 3 *Lmx1b*cKO mice). Two-way ANOVA with Welch's correction, *p<0.05, **p<0.001, and ***p<0.0001. Data are represented as mean ± SEM.

DOI: https://doi.org/10.7554/eLife.48788.005

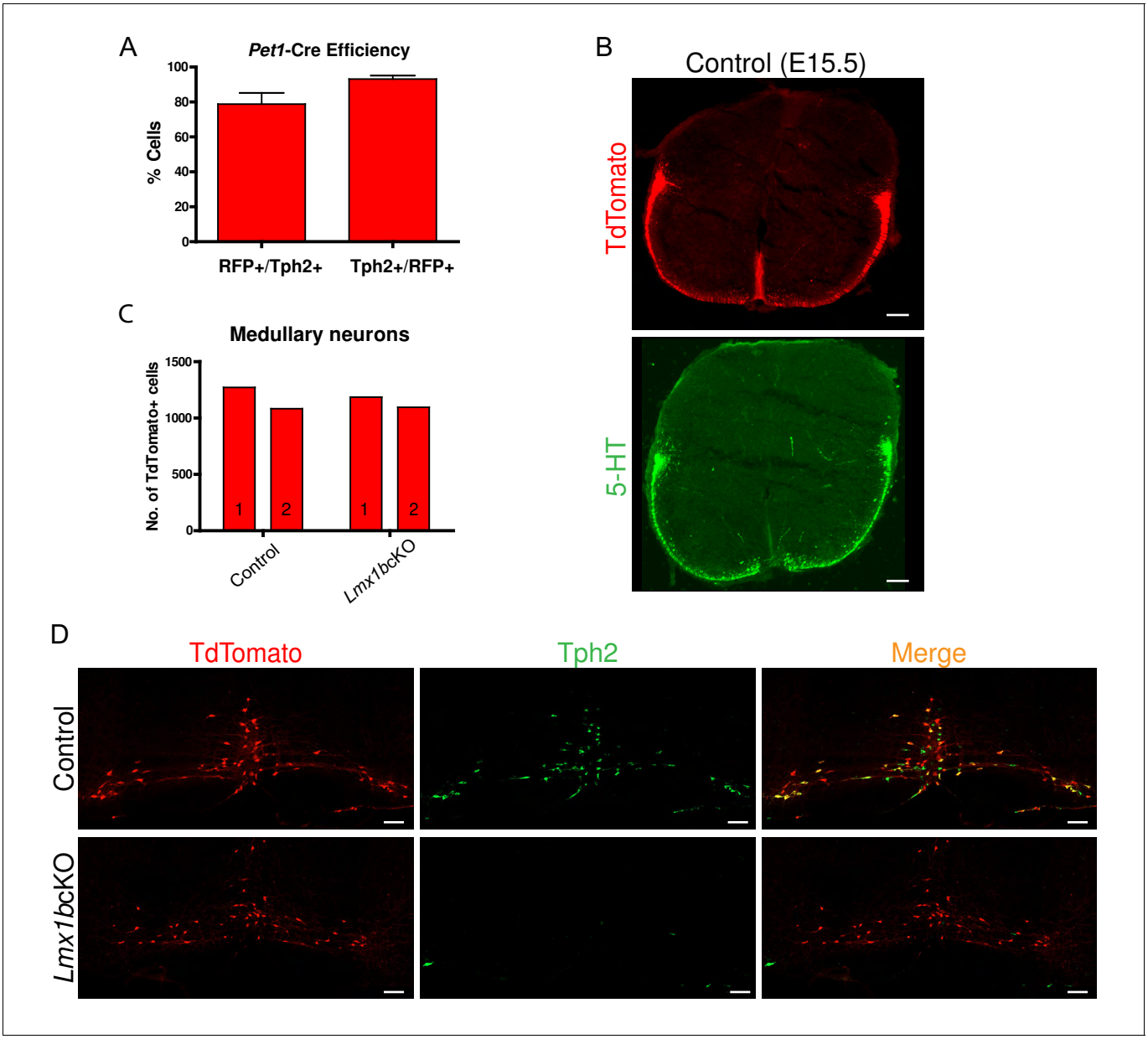

Figure 2—figure supplement 1. Conditional targeting of Lmx1b in the descending 5-HT projection pathway. (**A**) *Pet1-Cre* efficiency: 80% of Tph2+ cells expressed TdTomato+ (RFP+/Tph2+); 92% of TdTomato+ cells expressed Tph2 (Tph2+/RFP+) in medullary nuclei (n = 2 control mice). Data are represented as mean ± SEM. (**B**) TdTomato+ axon patterns in funiculi of the developing spinal cord aligned with 5- HT labeled axon patterns at E15.5 in controls (*coronal view*). Scale bars, 100 µm. (**C**) Comparable numbers of TdTomato+ medullary cells in *Lmx1b*cKO and control mice (n = 2 mice/genotype). (**D**) Few *Lmx1b*cKO TdTomato+ cell bodies expressed Tph2, a downstream target of Lmx1b. Scale bars, 100 µm.

DOI: https://doi.org/10.7554/eLife.48788.006

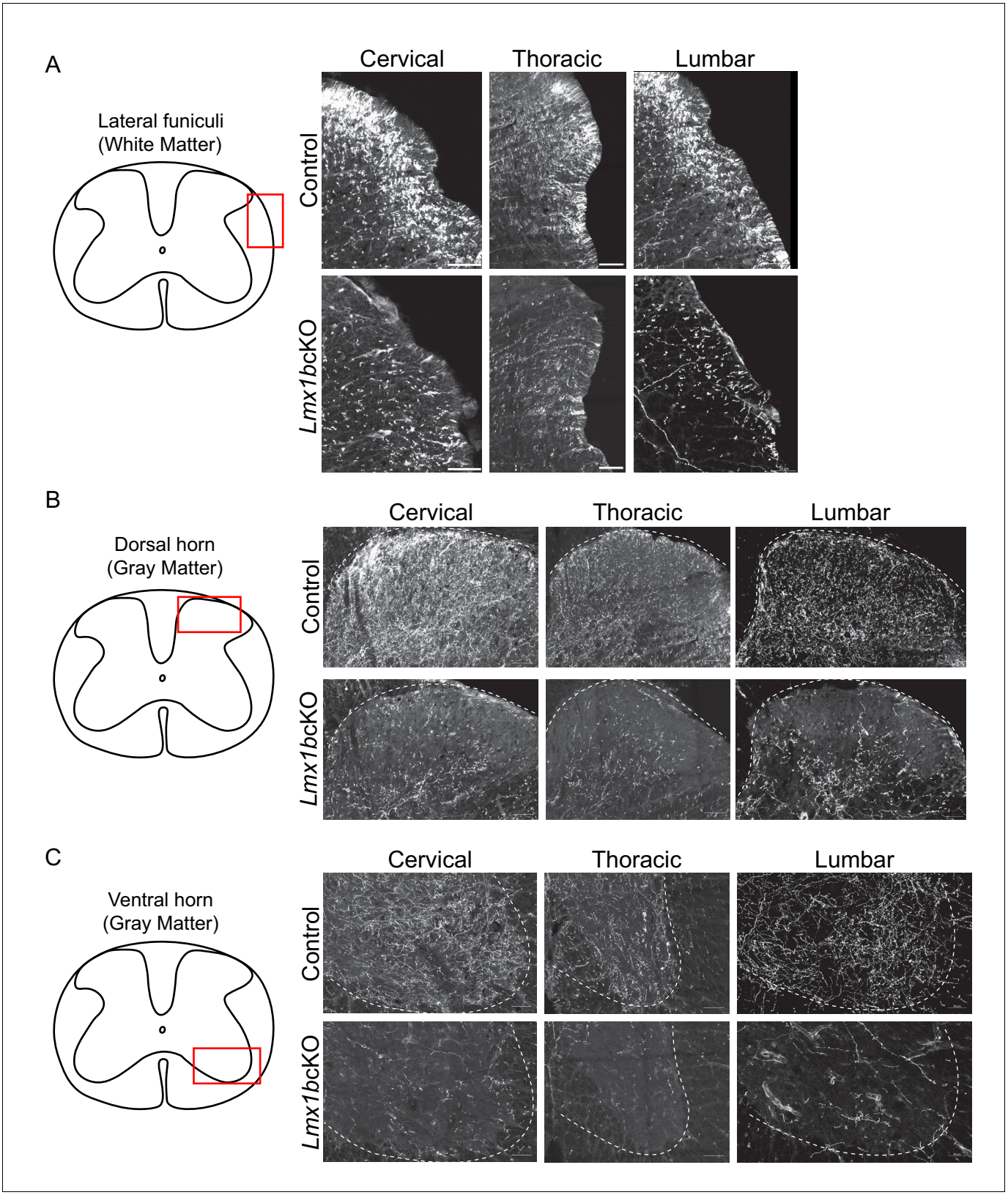

Figure 2—figure supplement 2. Progressive deficits of 5-HT axon fibers in Lmx1b deficient spinal cord white and gray matter. (**A-C**) Coronal sections immunolabeled using an anti-RFP antibody to TdTomato. *Lmx1b*cKO TdTomato^{+} axon deficits in spinal cord white matter funiculi (**A**), gray matter dorsal (**B**), and ventral (**C**) horns. Red box in diagram outlines area imaged (*right*). (n = 3, control; n = 3 *Lmx1b*cKO mice). Scale bars, 50 µm.
DOI: https://doi.org/10.7554/eLife.48788.007

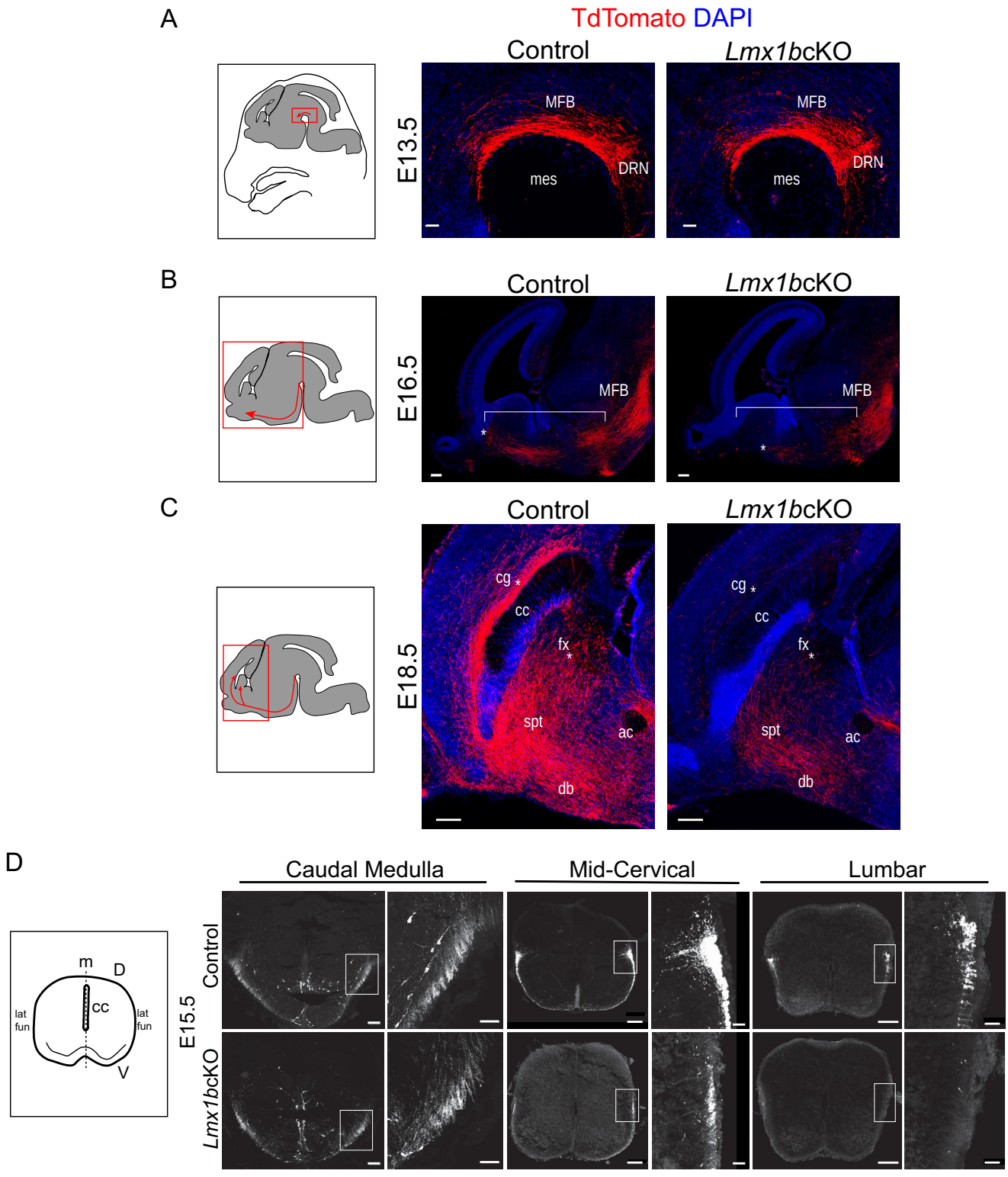

Figure 3. Initial axon outgrowth is delayed and selective pathway routing fails in Lmx1b deficient 5-HT neurons. (**A–C**) Immunolabeled TdTomato^{+} ascending axons in sagittal slices at different embryonic stages. Diagrams (*left*) show area of image (red box) presented for each time point. Arrows

Figure 3 continued on next page

Figure 3 continued

indicate direction of growing axons. E13.5 *Lmx1b*cKO axons exhibited similar ascending trajectories and densities as controls (**A**). E16.5 *Lmx1b*cKO axons did not extend as far (*asterisk*) and were less abundant (under bracket) compared to control axons (**B**). E18.5 *Lmx1b*cKO axons failed to fill multiple axon tracts (cg, fx; *asterisks*) compared to controls (**C**). Scale bars, 50 μm (**A**), 200 μm (**B,C**). DRN, *dorsal raphe nucleus*; MFB, *medial forebrain bundle*; mes, *mesencephalic flexure*; cg, *cingulum bundle*; fx, *fornix*; ac, *anterior commissure*; spt, *septum*; db, *diagonal band*; cc, *corpus callosum*. (**D**) Diagram (*left*) depicting coronal section of an embryonic spinal cord. TdTomato^{+} descending axons at E15.5 in control vs *Lmx1b*cKO embryos. *Lmx1b*cKO axons exit caudal medulla similar to controls but were severely reduced in funiculi at lower levels of the cord (mid-cervical and lumbar). Boxed region of lateral funiculi enlarged to the right of each image. Scale bars, 100 μm (low magnification), 50 μm (high magnification-medulla), 20 μm (high magnification- cervical/lumbar insets). Lat fun, *lateral funiculi*; cc, *central canal*; m, *midline*; D, *dorsal*; V, *ventral*.

DOI: https://doi.org/10.7554/eLife.48788.008

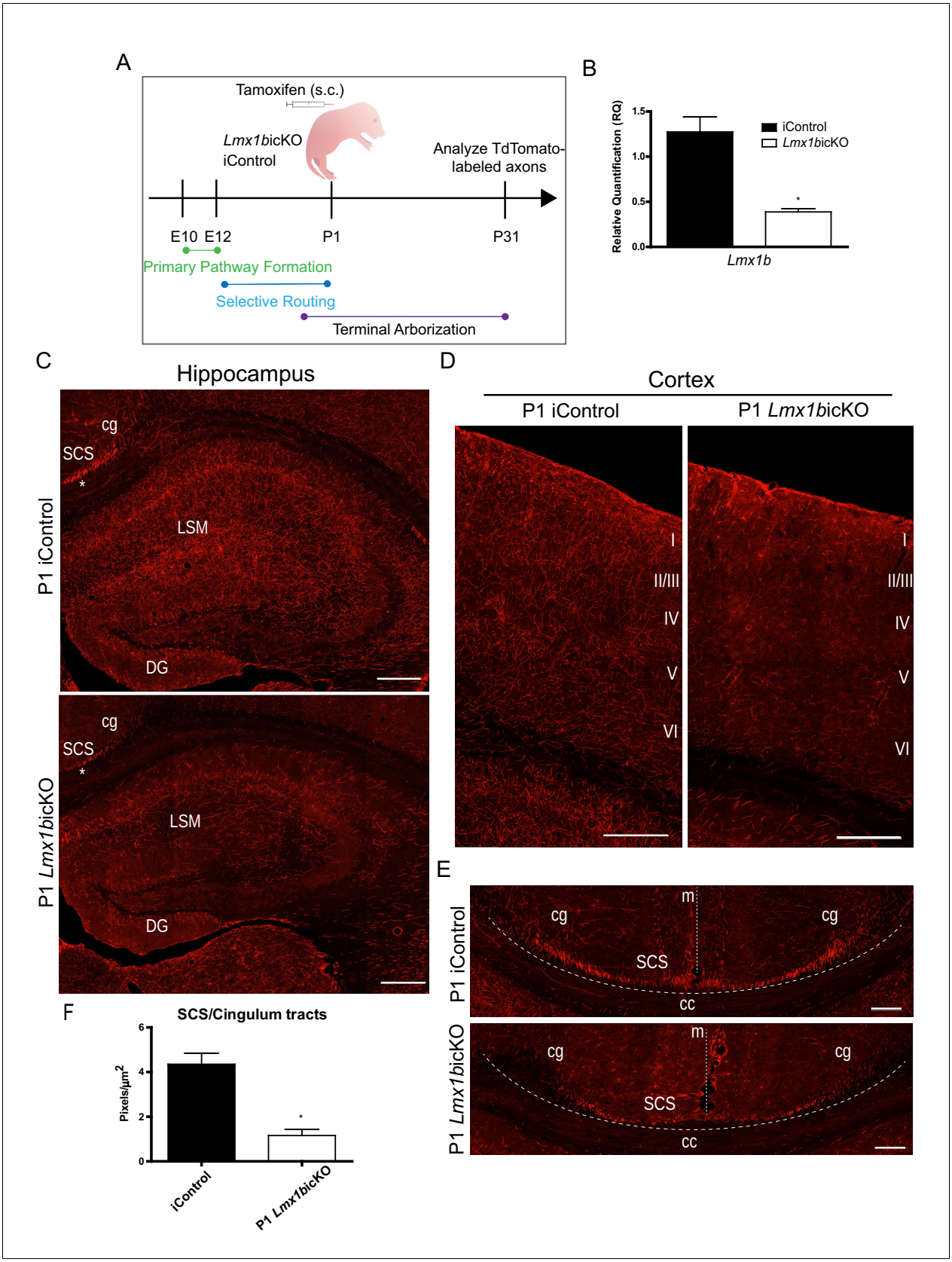

Figure 4. Lmx1b is temporally required for 5-HT projection pathway formation. (**A**) Schematic of tamoxifen-inducible approach to target *Lmx1b* at postnatal day (P)1. (**B**) RT-qPCR of flow sorted TdTomato^{+} neurons from postnatal targeted mice (n = 3, iControl; n = 4, *Lmx1b*icKO mice). Unpaired t-

Figure 4 continued on next page

Figure 4 continued

test with Welch's correction, *p<0.05. Data are represented as mean ± SEM. (**C**) Coronal sections of P1 targeted *Lmx1b*icKO hippocampus compared to iControls analyzed at P31. *, incomplete formation of SCS and cingulum in P1 targeted *Lmx1b*icKO brain. Scale bars, 200 μm. (**D**) Coronal sections of P1 targeted *Lmx1b*icKO cortex compared to iControls analyzed at P31. Scale bars, 200 μm. (**E**) Coronal sections at level of corpus callosum showing incomplete formation of major 5-HT axon routes, SCS and cingulum, in P1 targeted *Lmx1b*icKO forebrain compared to iControls (above dotted line). Scale bars, 100 μm. cg, *cingulum*; SCS, *supracallosal stria*; cc, *corpus callosum*; m, *midline*. (**F**) Quantification of axons within SCS and cingulum tracts (n = 3, iControl; n = 3, *Lmx1b*icKO mice). Unpaired t-test with Welch's correction, p=0.0112. Data are represented as mean ± SEM.

DOI: https://doi.org/10.7554/eLife.48788.009

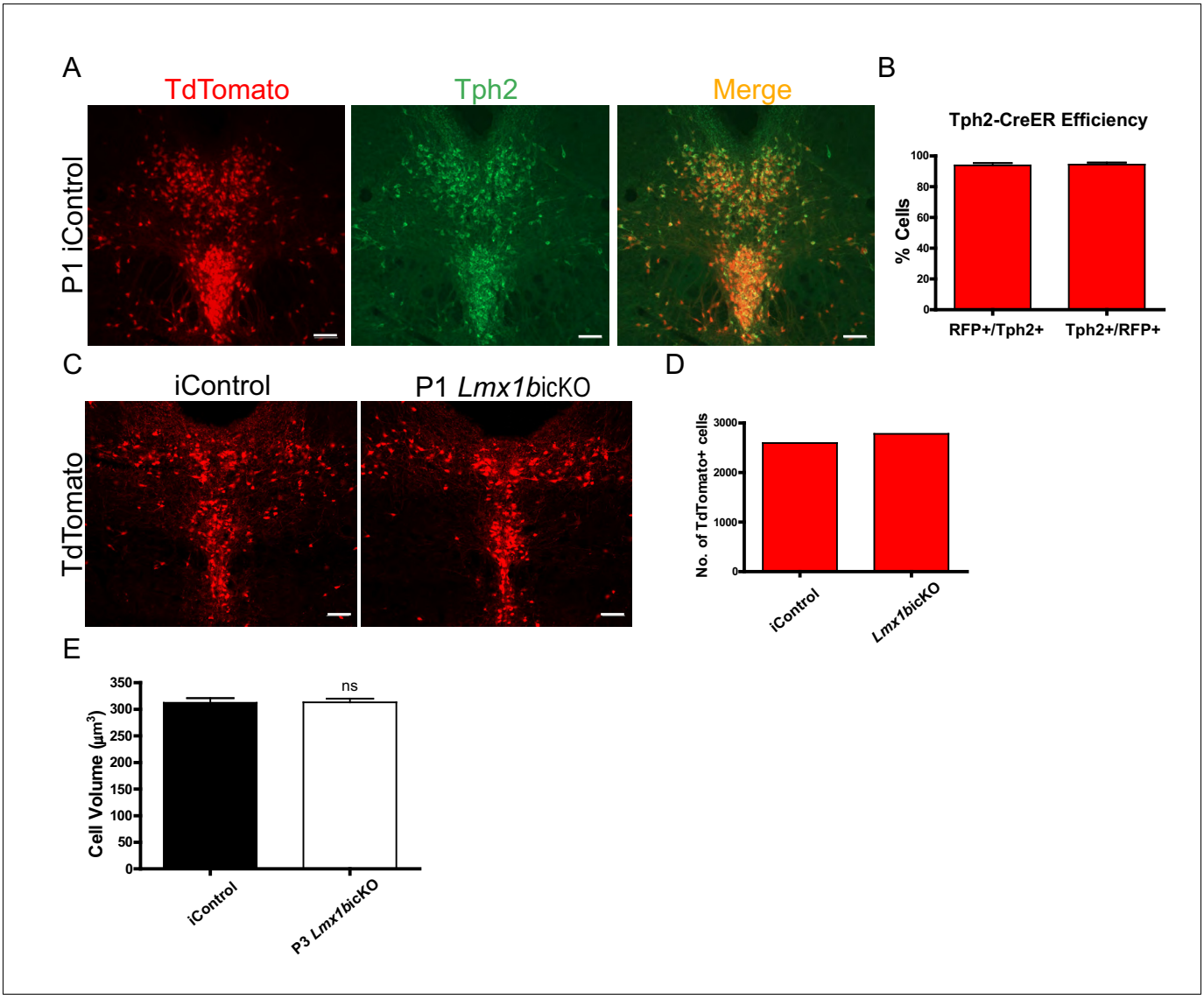

Figure 4—figure supplement 1. Efficiency of postnatal tamoxifen inducible targeting of Lmx1b. (**A**) TdTomato^{+} cells co- localized with serotonergic marker Tph2 in the DRN of iControl mice. Scale bars, 100 µm. (**B**) *Tph2-CreER* efficiency: 94% of TdTomato+ cells expressed Tph2 (Tph2+/RFP+) and 94% of Tph2+ cells expressed TdTomato+ (RFP+/Tph2+) in DRN/MRN/B9 nuclei (n = 4, iControl mice). Data are represented as mean ± SEM. (**C**) DRN of P1 targeted *Lmx1b*icKO and iControl mice. Scale bars, 100 µm. (**D**) Cell counts confirmed comparable numbers of TdTomato+ cells in *Lmx1b*icKO and iControl mice. (**E**) Normal cell body volume in postnatal targeted *Lmx1b*icKO mice (n = 464, control cells; n = 651, P3 *Lmx1b*icKO cells; p=0.9353). Unpaired t-test with Welch's correction. Data are represented as mean ± SEM.

DOI: https://doi.org/10.7554/eLife.48788.010

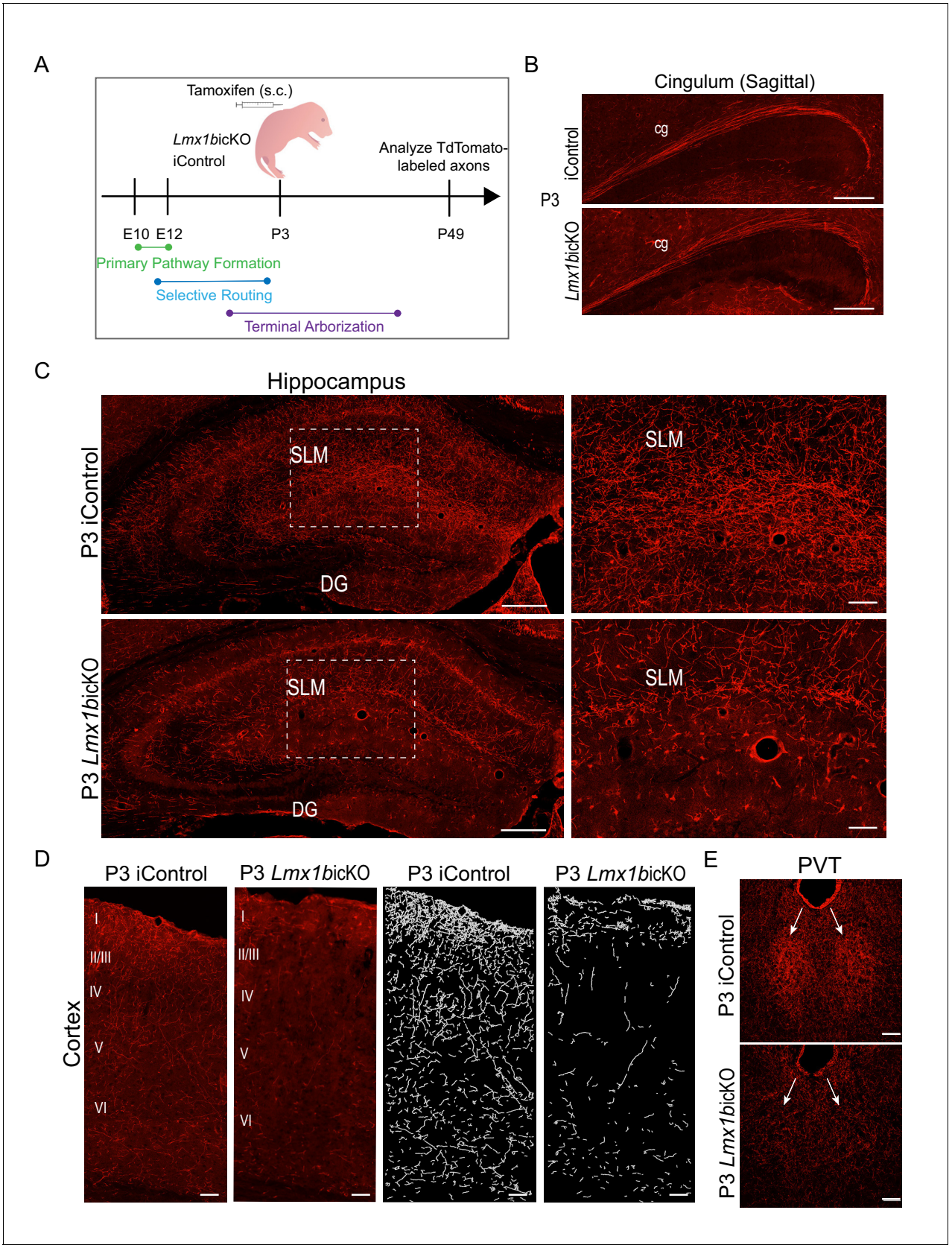

Figure 5. Lmx1b temporally controls postnatal 5-HT terminal arborization. (**A**) Schematic of tamoxifen inducible targeting of *Lmx1b* at postnatal day (P) 3. (**B**) Sagittal view of cingulum shows fully formed long-range axon routes in P3 targeted *Lmx1b*icKO mice compared to iControls. Scale bars, 200 µm.

Figure 5 continued on next page

Figure 5 continued

(**C**) Coronal sections of hippocampus in P3 targeted *Lmx1b*icKO mice compared to iControls. Dashed boxed region: higher magnification image at right highlighting reduced TdTomato$^+$ axons in *Lmx1b*icKO SLM. Scale bars, 200 μm (low magnification), 50 μm (high magnification). SLM, *stratum lacunosum moleculare*; DG, *dentate gyrus*. (**D**) Coronal sections of cortex of P3 targeted *Lmx1b*icKO mice compared to iControls. Imaris tracing; *right panels*. Scale bars, 100 μm. (**E**) Decreased TdTomato$^+$ arbors detected in P3 targeted *Lmx1b*icKO PVT compared to iControls (arrows). Scale bars, 50 μm.

DOI: https://doi.org/10.7554/eLife.48788.011

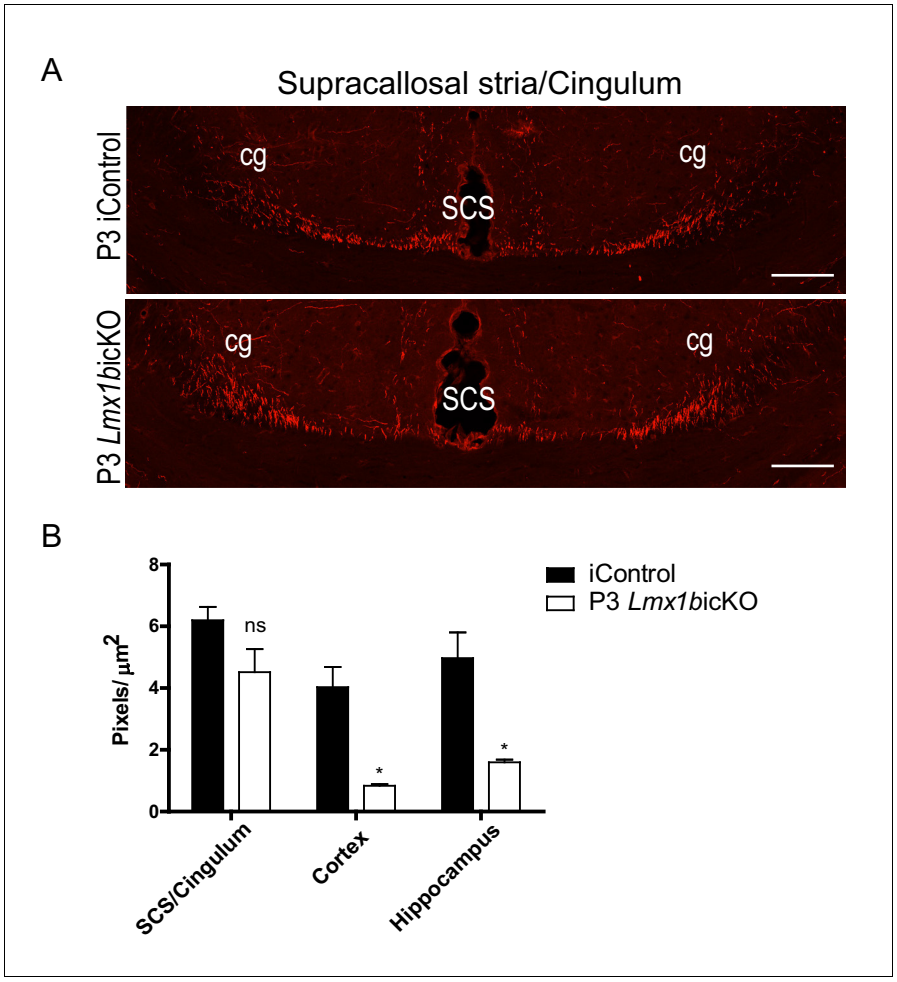

Figure 5—figure supplement 1. P3 targeted *Lmx1b*icKO mice display normal 5-HT axon routing but decreased 5-HT terminal arbors. (**A**) Coronal view of SCS and cingulum demonstrating complete formation of long-range axon routes in P3 targeted *Lmx1b*icKO mice compared to iControls. Scale bars, 100 µm. (**B**) Quantification of axons within SCS and cingulum tracts, cortex, and hippocampus of postnatal targeted P3 iControls and P3 *Lmx1b*icKO mice (n = 3, iControl; n = 3, *Lmx1b*icKO mice). Unpaired t-test with Welch's correction; axon tracts, p=0.1474; cortex, p=0.04; hippocampus, p=0.0277. Data are represented as mean ± SEM.

DOI: https://doi.org/10.7554/eLife.48788.012

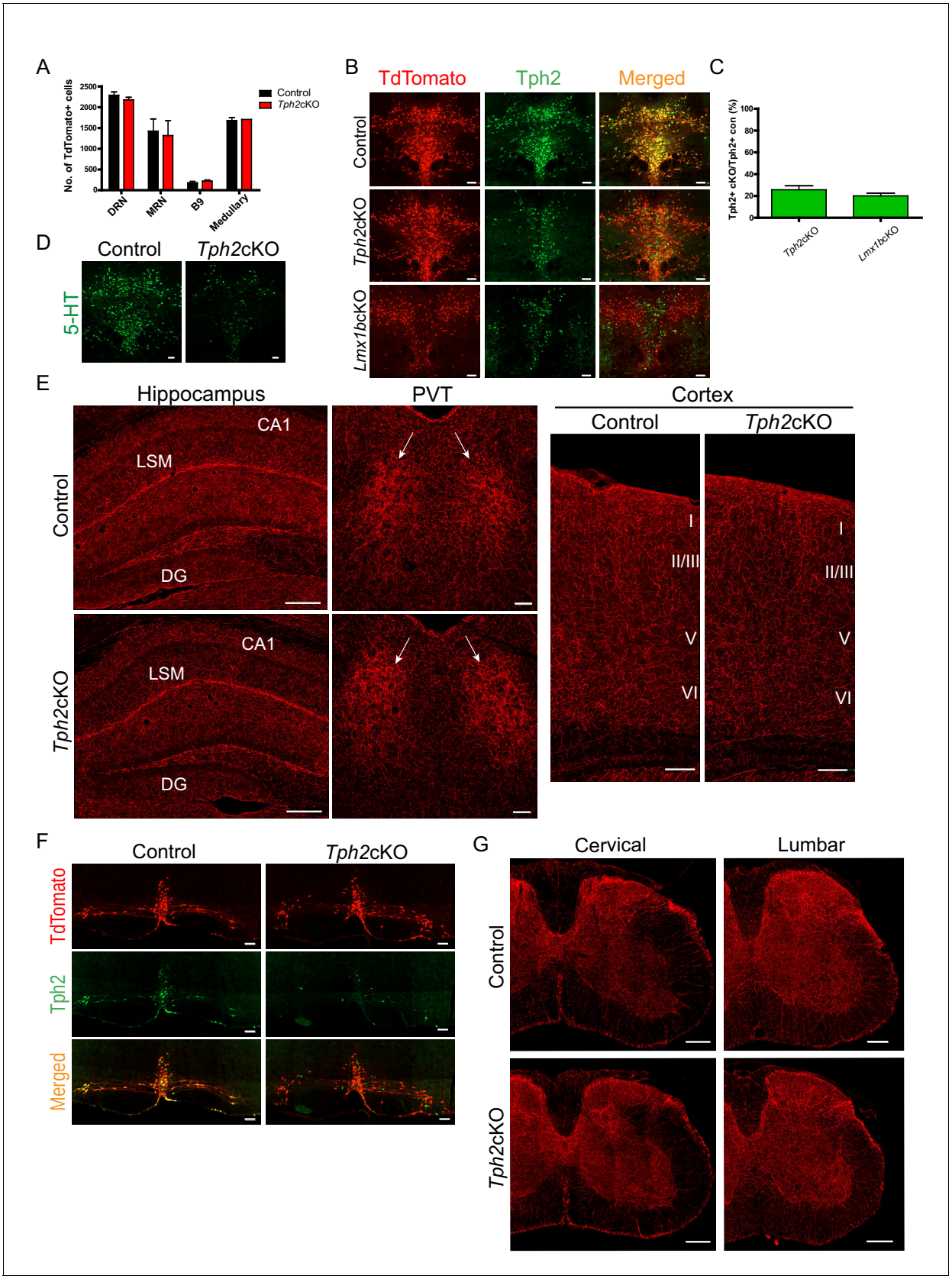

Figure 6. Specific targeting of 5-HT synthesis does not alter 5-HT arborization patterns. (**A**) Counts of TdTomato+ cells in each raphe nucleus of *Tph2*cKO mice did not differ from controls (n = 2 mice/genotype). Data are represented as mean ± SEM. (**B**) Comparable Tph2 knock-down in

Figure 6 continued on next page

Figure 6 continued

*Tph2*cKO and *Lmx1b*cKO mice. Scale bars, 100 μm. (**C**) Cell counts of residual Tph2$^+$ neurons in *Tph2*cKO and *Lmx1b*cKO mice expressed as a percentage (n = 2 mice/genotype). Data are represented as mean ± SEM. (**D**) Immunolabeling shows 5-HT was severely reduced in *Tph2*cKO mice. Scale bars, 100 μm. (**E**) Coronal forebrain sections showing no deficits of TdTomato$^+$ axon densities in *Tph2*cKO hippocampus, PVT, and cortex (n = 3 mice/genotype). LSM, lacunosum moleculare; DG, dentate gyrus; CA1 of hippocampus. Scale bars, 100 μm (PVT, cortex); 200 μm (hippocampus). (**F**) Co-immunolabeling for Tph2 and TdTomato in medullary neurons. Tph2 expression was severely reduced in medullary neurons of *Tph2*cKO mice. Scale bars, 50 μm. (**G**) No deficits of TdTomato$^+$ axons were present throughout the *Tph2*cKO spinal cord (n = 3 mice/genotype). Scale bars, 200 μm.

DOI: https://doi.org/10.7554/eLife.48788.013

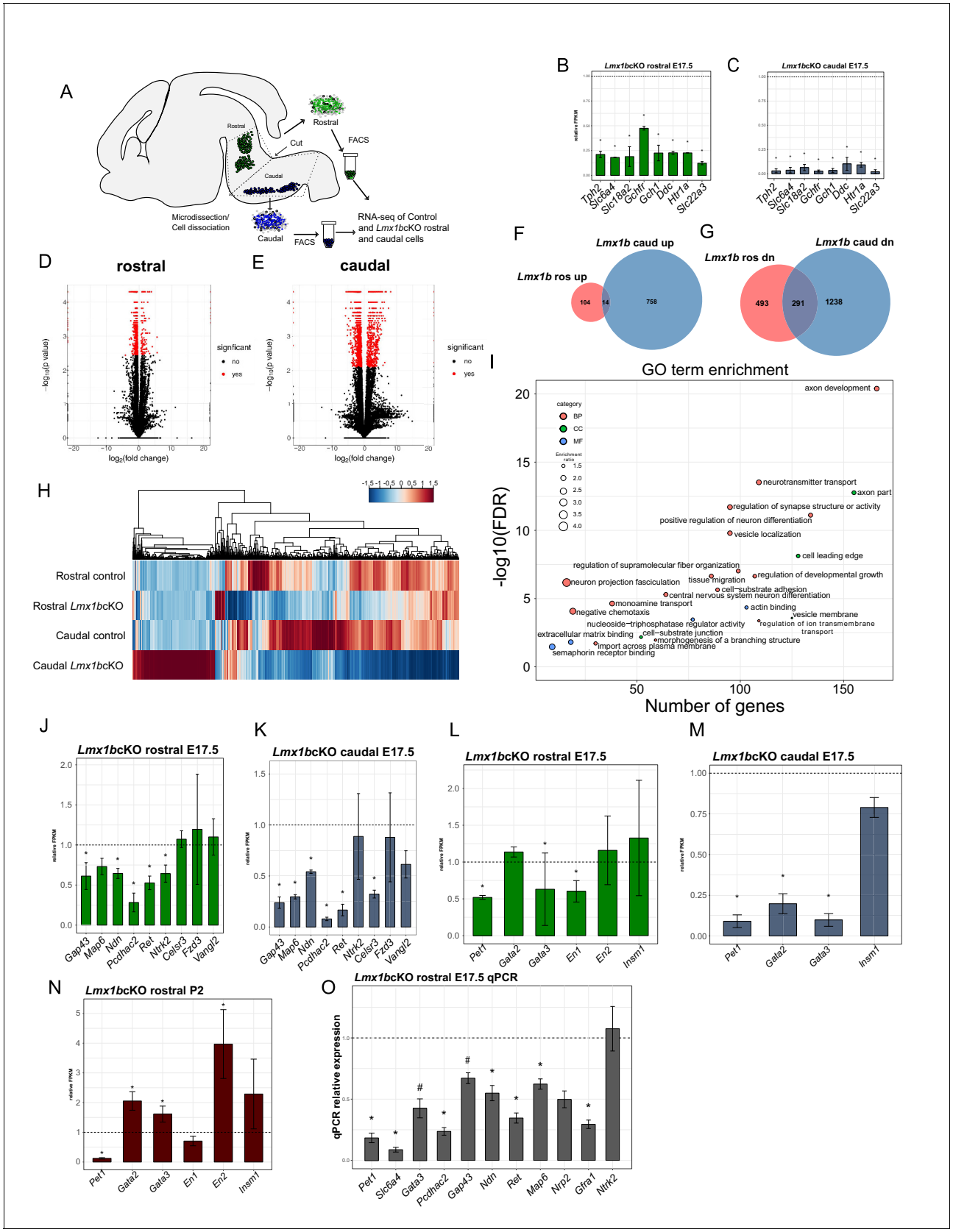

Figure 7. Ascending and descending Lmx1b regulated transcriptomes. (**A**) Schematic for dissection of E17.5 brain to isolate rostral and caudal 5-HT neurons genetically labeled by *Pet1-EYFP*. After dissection, EYFP^{+} neurons were flow-sorted separately and prepared for RNA-sequencing (n = 3,

Figure 7 continued on next page

Figure 7 continued

controls; n = 2 *Lmx1b*cKO embryos). (**B**) Relative expression level of 5-HT pathway genes in rostral control versus *Lmx1b*cKO 5-HT neurons. Control gene expression levels were normalized to one. * indicates FDR ≤ 0.05. Data are represented as mean ± SEM. (**C**) Relative expression level of 5-HT pathway genes in caudal control versus *Lmx1b*cKO 5-HT neurons. Control gene expression levels were normalized to one. * indicates FDR ≤ 0.05. Data are represented as mean ± SEM. (**D**) Volcano plot for rostral control versus *Lmx1b*cKO differential expression. Significantly altered genes are in red with ≥log2(1.5X) and FDR ≤ 0.05. (**E**) Volcano plot for caudal control versus *Lmx1b*cKO differential expression. Significantly altered genes are in red with ≥log2(1.5X) and FDR ≤ 0.05. (**F**) Venn diagram of genes upregulated in rostral and caudal *Lmx1b*cKO 5-HT neurons. (**G**) Venn diagram of genes downregulated in rostral and caudal *Lmx1b*cKO 5-HT neurons. (**H**) Heatmap of differentially-expressed genes in rostral and caudal *Lmx1b*cKO 5-HT neurons. (**I**) GO term enrichment of Lmx1b regulated genes. BP = biological process, CC = cellular component, MF = molecular function. GO terms were enriched with FDR ≤ 0.05. (**J**) Relative expression (FPKMs) of known 5-HT neuron axon-related genes in rostral *Lmx1b*cKO 5-HT neurons. Data are represented as mean ± SEM. (**K**) Relative expression (FPKMs) of known 5-HT neuron axon-related genes in caudal *Lmx1b*cKO 5-HT neurons. Data are represented as mean ± SEM. (**L**) Relative expression (FPKMs) of 5-HT GRN transcription factors in rostral *Lmx1b*cKO 5-HT neurons. Data are represented as mean ± SEM. (**M**) Relative expression (FPKMs) of 5-HT GRN transcription factors in caudal *Lmx1b*cKO 5-HT neurons. Data are represented as mean ± SEM. (**N**) Relative expression (FPKMs) of 5-HT GRN transcription factors in flow sorted TdTomato^{+} rostral *Lmx1b*cKO 5-HT neurons at postnatal day 2 (n = 3, controls; n = 4, *Lmx1b*cKO mice). Data are represented as mean ± SEM. (**O**) RT-qPCR verification of 5-HT GRN transcription factors and known axon-related genes from flow sorted rostral YFP+ *Lmx1b*cKO 5-HT neurons relative to control levels (n = 4 mice/genotype). * indicates p-value≤0.05, # indicates p<0.1, t-test with Welch's correction. Data are represented as mean ± SEM.

DOI: https://doi.org/10.7554/eLife.48788.014

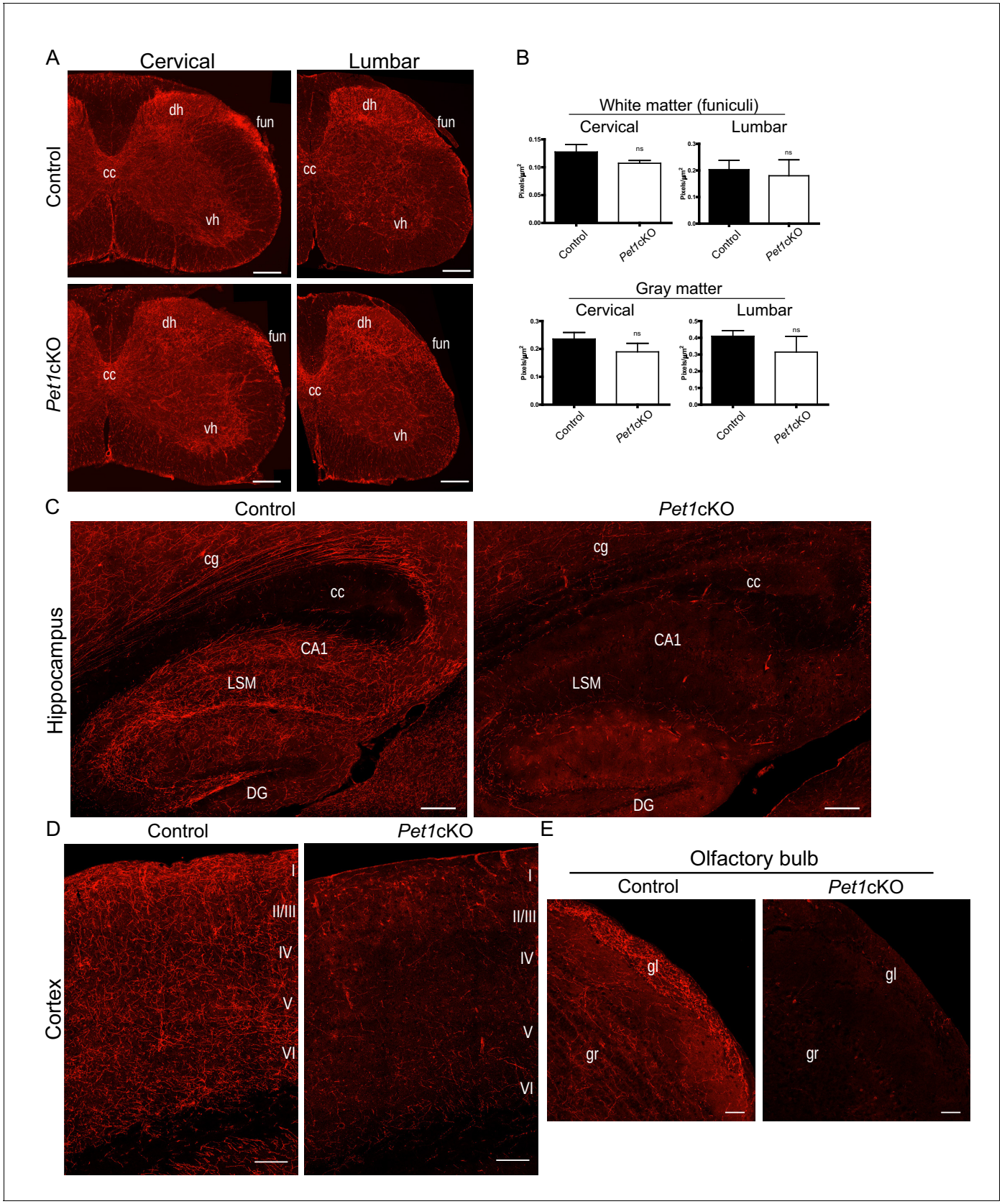

Figure 8. Distinct transcription factor requirements in the formation of ascending and descending 5-HT projection pathways. (**A**) TdTomato^{+} axon innervation in *Pet1*cKO vs control spinal cords in 3 month old mice. Coronal semi-section views of cervical and lumbar levels. Scale bars, 200 µm. cc,

Figure 8 continued on next page

Figure 8 continued

central canal; dh, *dorsal horn*; vh, *ventral horn*; fun, *funiculi*. (**B**) Quantification of TdTomato$^+$ axons (pixels/μm^2) in cervical and lumbar spinal cords (n = 3, controls; n = 3, *Pet1*cKO animals; Two-way ANOVA; white matter: cervical p=0.1372; lumbar p=0.6764; gray matter: cervical p=0.4440; lumbar p=0.1995). Data are represented as mean ± SEM. (**C**) Decreased TdTomato$^+$ arbors detected in *Pet1*cKO hippocampus compared to controls at 3 months of age. Scale bars, 200 μm, sagittal view. (**D**) Decreased TdTomato$^+$ arbors detected in *Pet1*cKO cortex compared to controls at 3 months of age. Scale bars, 100 μm, coronal view. (**E**) Decreased TdTomato$^+$ arbors detected in *Pet1*cKO olfactory bulb compared to controls at 3 months of age. Scale bars, 50 μm, sagittal view. cg, *cingulum*; cc, corpus callosum; LSM, *lacunosum moleculare*; DG, *dentate gyrus*; CA1 of hippocampus; gr, *granule layer*; gl, *glomerular layer*.

DOI: https://doi.org/10.7554/eLife.48788.015

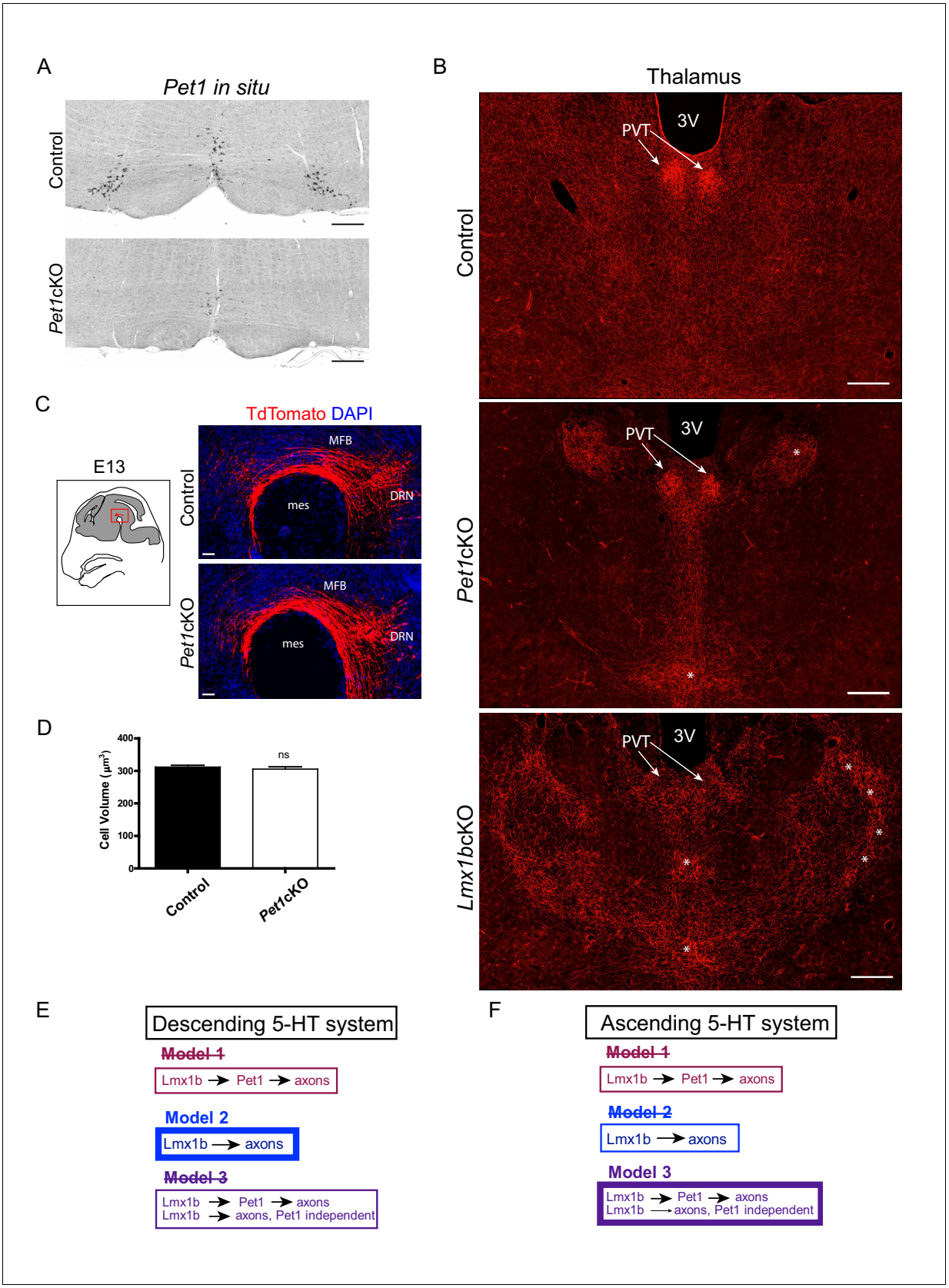

Figure 8—figure supplement 1. *Pet1*cKO and *Lmx1b*cKO mice exhibit distinct axon defects in thalamus. (**A**) *Pet1 ISH* shows *Pet1* was targeted in medullary neurons of *Pet1*cKO mice. Scale bars, 200 μm. (**B**) Distinctly different clumping pattern in *Pet1*cKO thalamus (*asterisks*) compared to

Figure 8—figure supplement 1 continued on next page

Figure 8—figure supplement 1 continued

*Lmx1b*cKO thalamus. Patterning in the PVT was normal in *Pet1*cKO mice (*arrows*). Scale bars, 200 μm. (**C**) No differences in early embryonic (E13.5) primary growth through the MFB in *Pet1*cKO embryos. Scale bars, 50 μm. (**D**) Cell volume analysis in *Pet1*cKO DRN revealed no significant difference in cell body size (n = 587 control cells; n = 549 *Pet1*cKO cells, p=0.4745). Compare to *Lmx1b*cKO cell volume, see ***Figure 1—figure supplement 1J***. Unpaired t-test with Welch's correction. Data are represented as mean ± SEM. (**E**) Scheme illustrating evidence-supported model for control of descending 5-HT axon development (Model 2). (**F**) Scheme illustrating evidence-supported model for control of ascending 5-HT axon development (Model 3).

DOI: https://doi.org/10.7554/eLife.48788.016

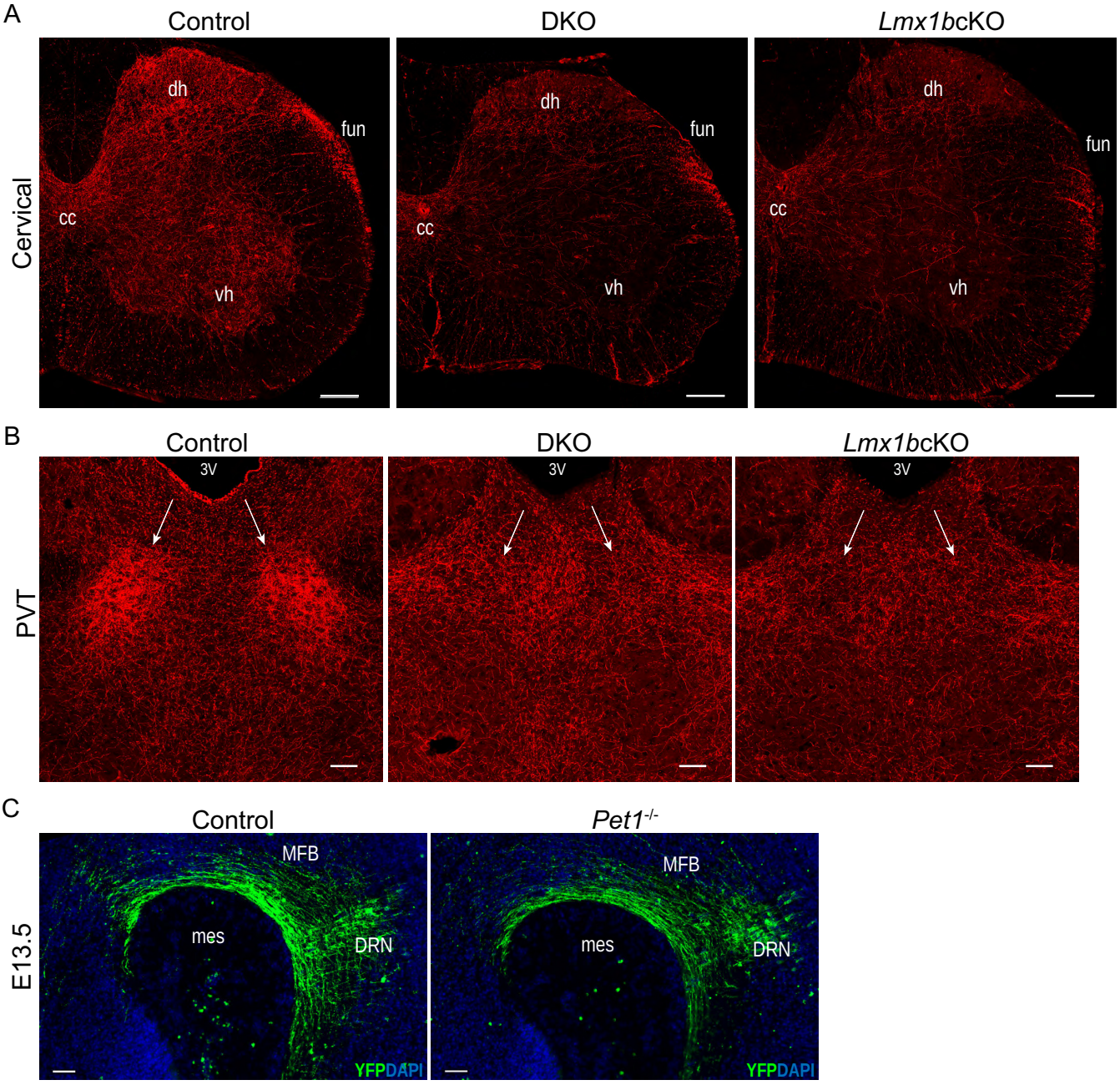

Figure 8—figure supplement 2. DKO and *Pet1*$^{-/-}$ analyses. (**A**) Similar 5-HT axons defects in spinal cord of DKO and *Lmx1b*cKO mice (n = 3 mice/genotype). Scale bars, 200 µm. cc, *central canal*; dh, *dorsal horn*; vh, *ventral horn*; fun, *funiculi*. (**B**) DKO PVT was unarborized similar to *Lmx1b*cKO PVT (n = 3 mice/genotype). Scale bars, 100 µm. PVT, *paraventricular nucleus of the thalamus*; 3V, *third ventricle*. (**C**) Immunolabeled YFP+ axons in *Pet1*$^{-/-}$ embryos at E13.5 showed no deficit in primary ascending axon growth through the MFB (n = 2 mice/genotype). Scale bars, 50 µm. MFB, *medial forebrain bundle*; mes, *mesencephalic flexure*.

DOI: https://doi.org/10.7554/eLife.48788.017

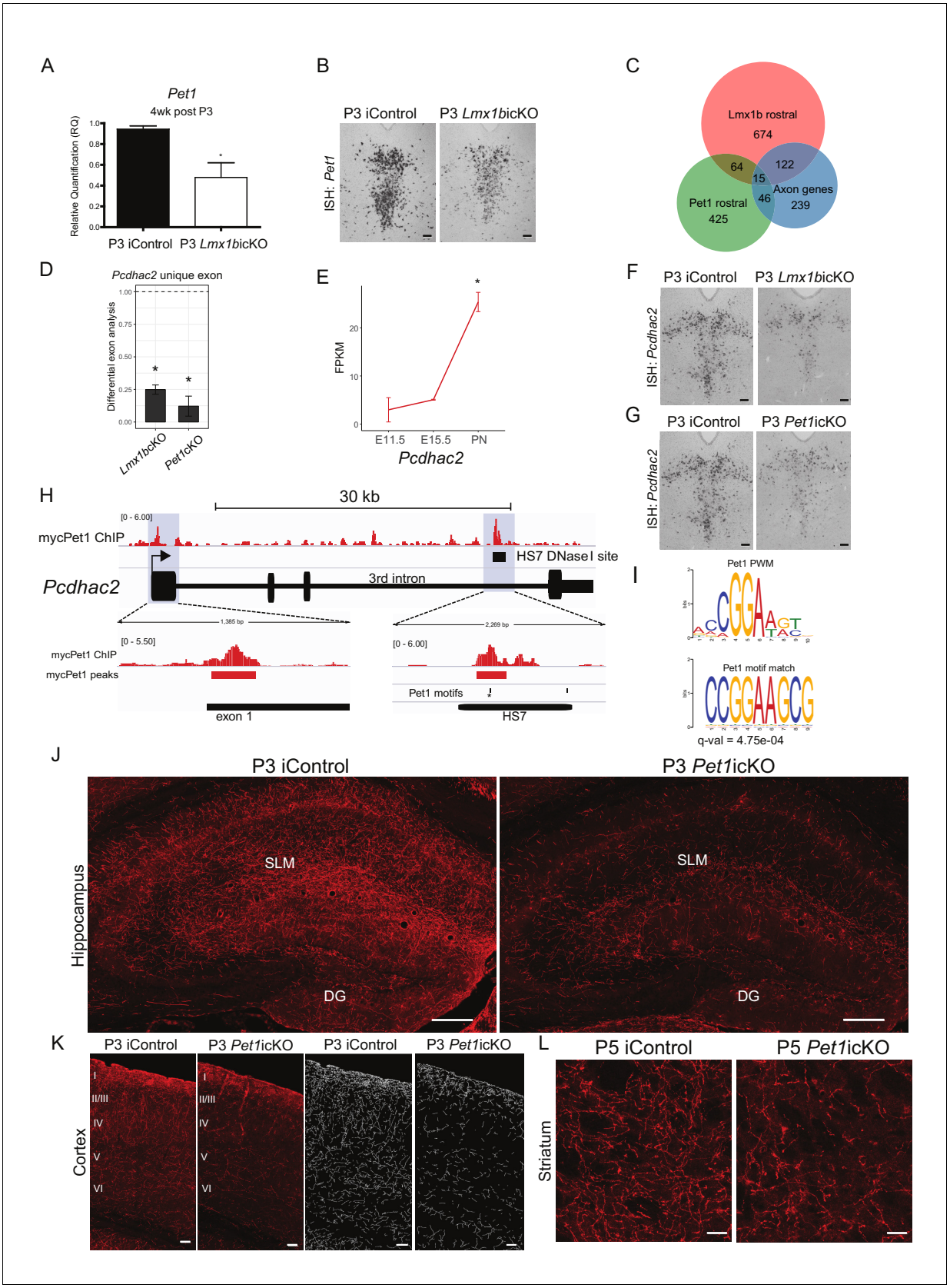

Figure 9. An ascending specific Lmx1b→Pet1 cascade controls stage specific 5-HT gene expression and postnatal terminal arborization. (**A**) RT-qPCR analysis of *Pet1* expression in flow sorted TdTomato^{+} neurons 4 weeks post P3 tamoxifen treatment (n = 3, iControl; n = 4, P3 *Lmx1b*icKO

Figure 9 continued on next page

Figure 9 continued

mice). Unpaired t-test with Welch's correction, *p<0.05. Data are represented as mean ± SEM. (**B**) *Pet1* in situ hybridization in P3 targeted *Lmx1b*icKO mice. Scale bars, 100 μm. (**C**) Venn diagram showing overlap of rostral Lmx1b and Pet1 regulated genes and the axon-related gene dataset. Lmx1b rostral: genes controlled by Lmx1b in rostral 5-HT neurons; Pet1 rostral: genes controlled by Pet1 in rostral 5-HT neurons; Axon genes: Lmx1b regulated rostral and caudal axon-related genes. (**D**) Relative expression of the unique *Pcdhac2* exon in rostral *Lmx1b*cKO and *Pet1*cKO 5-HT neurons. * indicates FDR $\leq$ 0.05. Data are represented as mean ± SEM. (**E**) Developmental expression profile of *Pcdhac2* in 5-HT neurons from E11.5 to early postnatal (PN). * indicates FDR $\leq$ 0.05. Data are represented as mean ± SEM. (**F**) *Pcdhac2* in situ hybridization at postnatal day 14 in P3 targeted *Lmx1b*icKO mice. Representative image from n = 3 mice/genotype. Scale bars, 100 μm. (**G**) *Pcdhac2* in situ hybridization at postnatal day 14 in P3 targeted *Pet1*icKO mice. *ISH* experiments done in parallel, iControl section is the same section in (**F**) and (**G**) to compare icKOs at the same tissue level. Representative image from n = 3 *Pet1*icKO mice. Scale bars, 100 μm. (**H**) Visualization of the *Pcdhac2* gene locus showing mycPet1 ChIP peaks at the TSS and 3rd intron (shaded) and matches to the known Pet1 motif. Zoomed regions of the significant mycPet1 binding sites are shown at the bottom. (**I**) The mycPet1 binding region located within the 3rd *Pcdhac2* intron DNAse I hypersensitivity site (HS7) contains a significant match to the known Pet1 position-weight matrix. TOMTOM q-value = 4.75×10^{-04}. (**J**) Decreased TdTomato^{+} arbors detected in P3 targeted *Pet1*icKO hippocampus compared to iControl mice. Scale bars, 200 μm. (**K**) Decreased TdTomato^{+} arbors detected in all layers of P3 targeted *Pet1*icKO cortex (Imaris tracing; *right panels*) compared to iControl mice. Scale bars, 50 μm. (**L**) Decreased TdTomato^{+} arbors in striatum of P5 targeted *Pet1*icKO mice. Scale bars, 20 μm. See also ***Figure 9—figure supplement 1F***.

DOI: https://doi.org/10.7554/eLife.48788.018

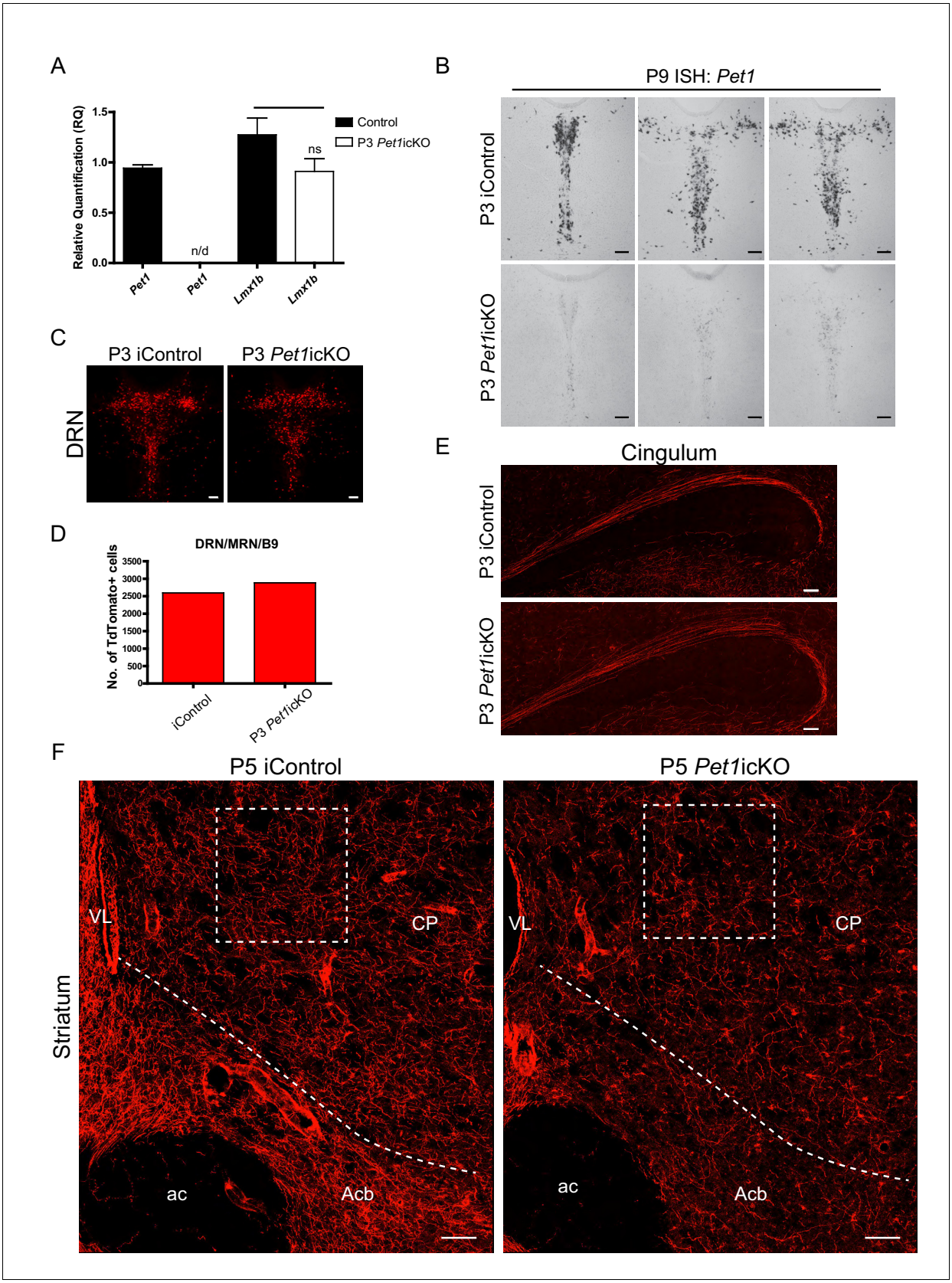

Figure 9—figure supplement 1. Lmx1b→Pet1 cascade acts postnatally to control 5-HT terminal arborization. (**A**) RT-qPCR of flow sorted TdTomato^{+} cells in P3 targeted *Pet1*icKO mice at 4 weeks of age. *Pet1* was not detected by qPCR in flow sorted cells. *Lmx1b* was not significantly regulated by

Figure 9—figure supplement 1 continued on next page

Figure 9—figure supplement 1 continued

Pet1 (p=0.1791) (n = 3, iControl; n = 3, *Pet1*icKO mice). Unpaired t-test with Welch's correction, *p<0.05. Data are represented as mean ± SEM. (**B**) *Pet1 ISH* confirmed *Pet1* targeting in the DRN. Scale bars, 100 μm. (**C, D**) Similar numbers of TdTomato^{+} cells were counted in P3 *Pet1*icKO and P3 iControl mice. Scale bars, 100 μm. (**E**) Long-range cingulum route was fully formed in P3 targeted *Pet1*icKO mice. Scale bars, 100 μm. (**F**) Analysis of TdTomato+ arbors in P5 targeted *Pet1*icKO mice revealed continuing requirement for Pet1 late-stage arborization in the striatum. Boxed regions presented in ***Figure 8L***. Scale bars, 50 μm. CP, *caudate putamen*; Acb, *nucleus accumbens*; ac, *anterior commissure*; VL, *lateral ventricle*.

DOI: https://doi.org/10.7554/eLife.48788.019